

# Effect of distorted illumination waves on coherent diffraction microscopy

Yoshiki Kohmura,<sup>a)</sup> Yoshinori Nishino, and Tetsuya Ishikawa  
*Spring-8/RIKEN, 1-1-1 Kouto, Sayo-cho, Sayo-gun, Hyogo 679-5198, Japan*

Jianwei Miao

*Department of Physics and Astronomy and California Nanosystems Institute, University of California, Los Angeles, California 90095-1547*

(Received 20 May 2005; accepted 7 November 2005; published online 30 December 2005)

Coherent diffraction microscopy requires a well-defined illumination wave such as a plane wave on a specimen. Experimentally, a small pinhole or a focused beam is often used to reduce the illumination area but they unavoidably distort the waves. The distortion of the illumination wave causes artifacts in the phase retrieval of oversampled diffraction patterns. Using computer simulations, we searched for the conditions where strong artifacts arise by changing the Fresnel number, pinhole size, alignment error and photon statistics. The experimental setup with Fresnel number of around 1 and smaller than 1 realized a small reconstruction error when the pinhole radius is larger than a few times the specimen size. These conditions are suitable for the rotation of specimens for the three-dimensional (3D) observations. Such investigation will have an impact in the design of coherent diffraction microscopes for the 3D characterization of nanoscale materials and biological systems using the third generation synchrotron radiation and future x-ray free-electron lasers. © 2005 American Institute of Physics. [DOI: 10.1063/1.2149499]

## I. INTRODUCTION

Coherent x-ray-diffraction microscopy using the third generation synchrotron radiation has emerged as an important technique to quantitatively image nanoscale materials and biological systems in two and three dimensions.<sup>1-8</sup> To date, a highest resolution of 7 nm has been achieved.<sup>9</sup> With the prospects of brighter x-ray sources such as energy recovery linacs<sup>10,11</sup> and x-ray free-electron lasers,<sup>12-14</sup> near atomic resolution will be possible for radiation hard nanoscale materials.

The principle of coherent diffraction microscopy is based upon the oversampling method with iterative algorithms. It was first suggested by Sayre that sampling the diffraction intensity at a frequency finer than the Nyquist interval may provide the phase information.<sup>15</sup> Based upon the argument of the number of correlated intensity points versus the number of unknown variables, Miao *et al.* proposed a theoretical explanation to the oversampling method.<sup>16</sup> The oversampling ratio  $\sigma$  was introduced to characterize the degree of oversampling. When  $\sigma > 2$ , the number of correlated intensity points is more than the unknown variables and the phases are in principle encoded inside the diffraction intensity,<sup>16</sup> which can be retrieved by using iterative algorithms developed by Gerchberg and Saxton<sup>17</sup> and Fienup.<sup>18</sup>

The oversampling method with iterative algorithms requires a well-defined illumination wave such as a plane wave. Although there are attempts for other types of illumination wave, such as waves containing cylindrical phase curvature,<sup>5</sup> this paper describes the problems caused by the distorted illumination waves in phase retrieval. Although a circular pinhole is usually used in coherent x-ray-diffraction

microscopy for reducing the illumination area and the background scattering, the Fresnel diffraction effect due to the pinhole is neglected in the analysis. The distortion of the illumination wave due to the Fresnel diffraction can seriously affect the quality of phase retrieval from the oversampled diffraction patterns. It can cause strong artifacts in the retrieved images if a plane wave is assumed for the iterative algorithm. The solution for avoiding artifacts was searched by qualifying the phase retrieval as a function of the Fresnel number, pinhole size, alignment error, and photon statistics. This paper will give insight to the design of the coherent imaging experiments free from the artifacts produced by the distorted illumination wave.

## II. INHOMOGENEITY OF ILLUMINATION WAVE FIELD DUE TO FRESNEL DIFFRACTION

To retrieve the electron-density distribution from an oversampled diffraction pattern, a well-defined wave field on the specimen, such as a plane wave, is needed. A high flux onto the specimen is also desirable for achieving good statistics. The property of Fresnel illumination is dependent on the square of the ratio between the pinhole radius ( $r$ ) and the first Fresnel zone radius ( $r_1$ ). The Fresnel number,  $F_N = r^2/\lambda L = (r/r_1)^2$ , is a good indicator of the illumination, where  $\lambda$  is the wavelength and  $L$  is the distance between the pinhole and the specimen.

In the far-field case (i.e.,  $F_N \ll 1$ ), only one zone affects the phase and amplitude of the wave field at the near-axis specimen and quasiplane wave is easily achieved at specimen position. However, the beam size at the specimen position is enlarged. For an Airy pattern of a circular pinhole, the radius of the first minimum ( $\omega L$ ) is known to be

<sup>a)</sup>Electronic mail: kohmura@spring8.or.jp

$$\omega L = 0.61\lambda L/r, \quad (1)$$

where  $\omega$  is the angle of the first minimum.<sup>19</sup> The x-ray flux incident on the specimen is decreased inversely proportional to the square of the distance ( $L$ ) between the pinhole and the specimen, causing the diffracted intensity from the specimen to be reduced. In the near-field case ( $F_N > 1$ ),  $r > r_1$  is satisfied. The opening of the pinhole contains a number of zones interfering destructively.<sup>19</sup> This results in the complex phase and amplitude distribution of the wave field at the near-axis specimen.

The diffraction from the pinhole and the specimen interferes each other as well. The observed angular distribution at the detector plane,  $\Phi_i(q_x, q_y)$ , is expressed by the following convolution integral:

$$\Phi_i(q_x, q_y) = \Phi_i(q_x, q_y) * T(q_x, q_y), \quad (2)$$

where  $*$  represents the convolution, and  $\Phi_i(q_x, q_y)$  and  $T(q_x, q_y)$  represent the angular distributions of the diffraction from the pinhole and from the specimen.<sup>20</sup>  $\Phi_i(q_x, q_y)$  is a function of the distance  $L_d$  (distance between pinhole and detector). By placing the specimen in the extreme near field from the pinhole ( $F_N = \infty$ ), the specimen and pinhole can be defined as a single object.

### III. METHOD OF SIMULATION

A plane wave of 8 keV x-ray ( $\lambda = 1.55 \text{ \AA}$ ) was simulated to illuminate a circular pinhole with a radius between 3 and 25  $\mu\text{m}$ . The thickness of the pinhole and the scattering from the edge roughness of the pinhole were not taken into account in the simulation. The transmissivities of 100% and 0% were assumed inside and outside the pinhole. The wave field with complex amplitude downstream of the pinhole was calculated using the Fresnel-Kirchhoff integral. The calculation was done for various Fresnel numbers ( $F_N$ ) corresponding to various distances between the pinhole and the specimen ( $L$ ). Complex electron-density distribution [ $\rho_e(r)$ ] and a complex wave field at the specimen position [ $\Phi_{in}(r)$ ] were assumed. As the diffraction angle is extremely small in x-ray experiments with small pinholes, the inclination factor, describing the angular dependence of the amplitude variation of the secondary waves, was assumed to be a constant over the whole area of the pinhole. Since the transmitted beam through the specimen was usually blocked by a beamstop, it was not considered in the diffraction intensity.

A silicon cluster with a random network structure was used as the specimen which consists of  $2.821 \times 10^{10}$  atoms in a volume of  $4.4 \times 4.4 \times 0.5 \mu\text{m}^3$  (88 pixels  $\times$  88 pixels  $\times$  10 pixels). The pixel size is 50 nm. The thickness was chosen to get an average density of the specimen, 0.14  $\text{g/cm}^3$ , which is close to a realistic specimen. The modeled silicon particles are shown in Fig. 1. For a specimen composed of a single element, the powerful constraint of non-negativity can be applied which prevents the stagnation problem encountered during reconstruction for complex objects (with complex scattering factor).<sup>21</sup>

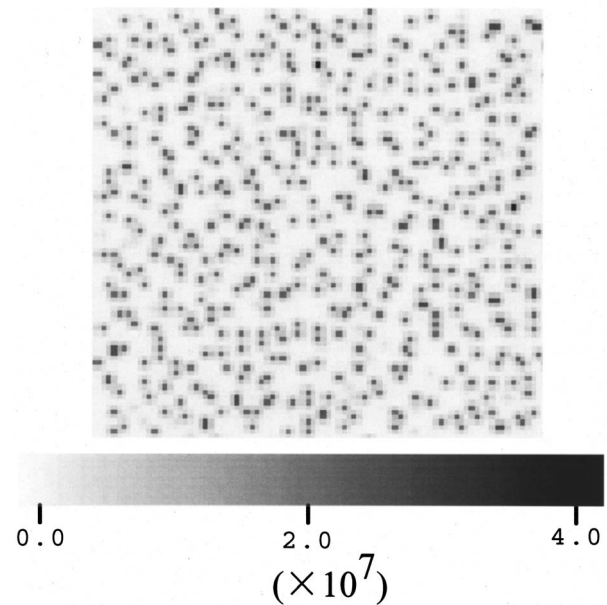


FIG. 1. A modeled silicon particle consisting of  $2.821 \times 10^{10}$  atoms in a random network structure within a volume of  $4.4 \times 4.4 \times 0.5 \mu\text{m}^3$ .

Electron density of the specimen was retrieved from the simulated diffraction pattern using the iterative hybrid input/output error-reduction algorithm.<sup>17,18</sup> The quality of the reconstruction was examined by an  $R$  factor.

$$R = \sqrt{\sum_{\mathbf{x} \in S} [\rho_o(\mathbf{x}) - \rho_r(\mathbf{x})]^2 / \sum_{\mathbf{x} \in S} [\rho_o(\mathbf{x}) + \rho_r(\mathbf{x})]^2}, \quad (3)$$

where  $\rho_o$  is the original image,  $\rho_r$  the reconstructed one, and  $S$  represents the region inside the support. The convergence of the reconstruction was examined by the reconstruction error defined as<sup>17</sup>

$$E_r = \sqrt{\sum_{\mathbf{x} \in S} [\rho(\mathbf{x})^2] / \sum_{\mathbf{x} \in S} [\rho(\mathbf{x})^2]}. \quad (4)$$

In coherent diffraction microscopy, the oversampling ratio ( $\sigma$ ) is an important parameter defined as<sup>16</sup>

$$\sigma = [\text{volume (electron-density region)} + \text{volume (no density region)}] / \text{volume (electron-density region)}. \quad (5)$$

The iterative algorithm was designed so that the density outside the support gradually approaches 0.<sup>17,18</sup> In the modeling, an area of  $2048 \times 2048$  pixels in both real and reciprocal spaces was simulated. The support was chosen to be a tight one with the size of  $88 \times 88$  pixels, which is the real envelop of the specimen (Fig. 1). Thereby the oversampling ratio was fixed to be  $\sigma = 23 \times 23$ . This ratio is large enough for fast convergence using the oversampling method.<sup>16</sup> All the diffraction patterns were centrosymmetrized before the reconstruction. The convergence curves were averaged five reconstructions with different initial seeds and the same number of 4500 iterations. The effects due to the Fresnel illumination conditions were examined without consideration of the missing center problem.<sup>22,23</sup>

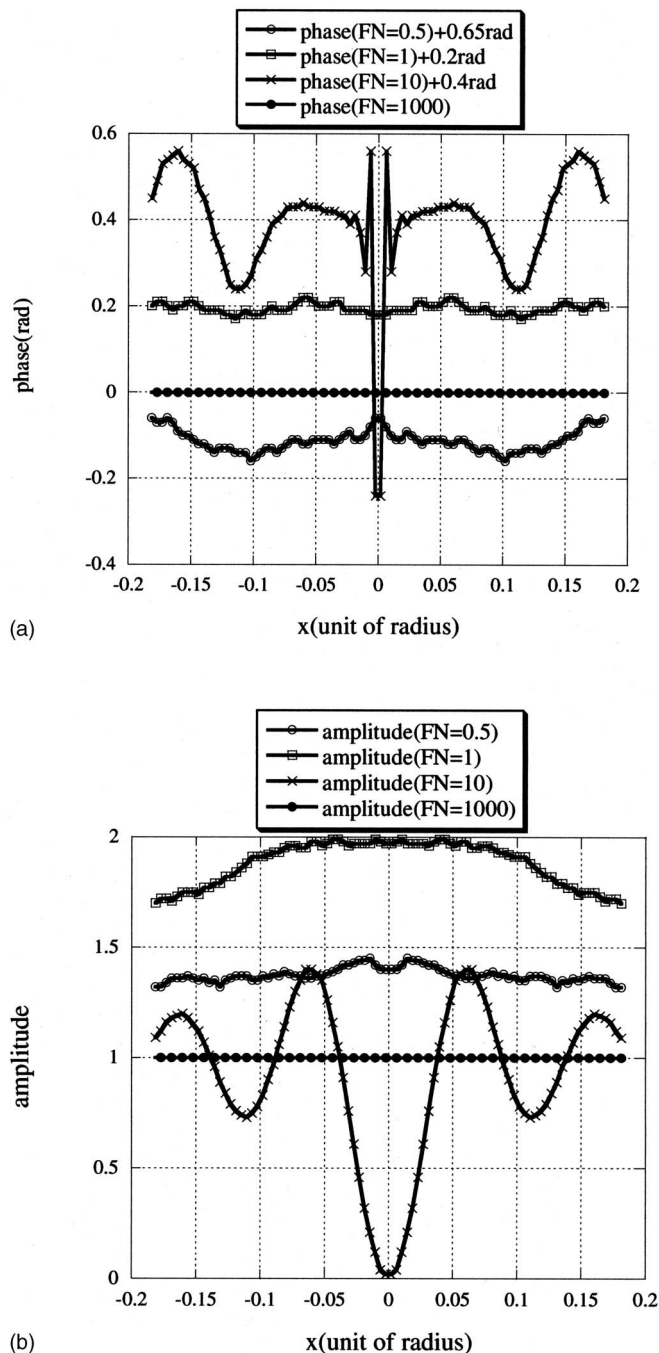


FIG. 2. One-dimensional amplitude and phase profiles perpendicular to the optical axis. A plane-wave illumination was assumed. Profiles at specimen plane were simulated with different Fresnel numbers of 0.5, 1, 10, and 1000, respectively. The calculation was done within the size of the specimen. For clarity, the phase profiles were shifted by arbitrary offsets.

#### IV. RESULTS OF SIMULATION

##### A. Correlation of reconstruction accuracy and uniformity of illuminating field with the Fresnel number

The Fresnel diffraction from a pinhole affects the uniformity of the illumination wave at the specimen position. One-dimensional amplitude and phase profiles along the optical axis were calculated within the size of the specimen (i.e.,  $4.4 \times 4.4 \mu\text{m}^2$ ). The pinhole radius was fixed to be  $12 \mu\text{m}$ , 2.7 times larger than the specimen size. Figure 2 and Table I

TABLE I. The quality of reconstruction (*R* factor and reconstruction error) as a function of the standard deviations of amplitude within the size of the specimen for various Fresnel numbers. The pinhole radius of  $12 \mu\text{m}$  and the oversampling ratio  $\sigma=23 \times 23$  were used. Each reconstruction was terminated after 4500 iterations. The Fresnel number of infinity represents the simulation without a pinhole.

$F_N$	Deviation (ampl, normalized)	<i>R</i> factor	Reconstruction error
0.5	0.026	0.0097	0.008
1	0.13	0.036	0.003
2	0.33	0.25	0.01
10	0.19	0.096	0.07
100	0.055	0.078	0.03
1000	0.000 046	0.0008	0.0002
$\infty$ (No pinhole)	0	0.0007	0.0002

show that the illuminating wave field is almost completely flat when  $F_N=1000$ . They are relatively flat when  $F_N \leq 1$ .  $F_N=1000$  represents the extreme proximity case of the specimen.

The quality of reconstruction versus uniformity of the illumination wave for various Fresnel numbers was examined as summarized in Table I. Using reconstruction error and *R* factor as indicators, the best convergences were achieved when  $F_N=1000$ . Good convergence was achieved when  $F_N \leq 1$  (Fig. 3). These results coincide with the small deviations of the phase and the amplitude observed when  $F_N=1000$  and  $F_N \leq 1$ . In the case of  $F_N \leq 1$ , only one Fresnel zone is included in the opening of the pinhole and the illumination wave is almost flat if the specimen is small enough. This is why relatively good convergence is observed and no obvious artifacts are seen in the reconstructed image for  $F_N \leq 1$  [Fig. 4(a)]. When FN is between 2 and 100, multiple Fresnel zones interfere destructively and the uniformity of the illumination wave becomes poor; thereby, the reconstructions were not as good. When  $F_N$  is an even number, the

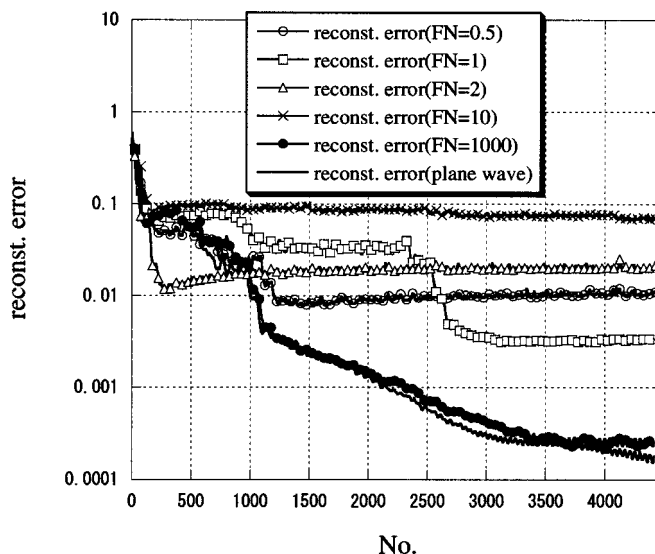


FIG. 3. The reconstruction error as a function of the number of iterations. The convergence of 4500 iterations is shown for  $F_N=0.5, 1, 2, 10, 1000,$  and  $\infty$  (i.e., plane wave), respectively.

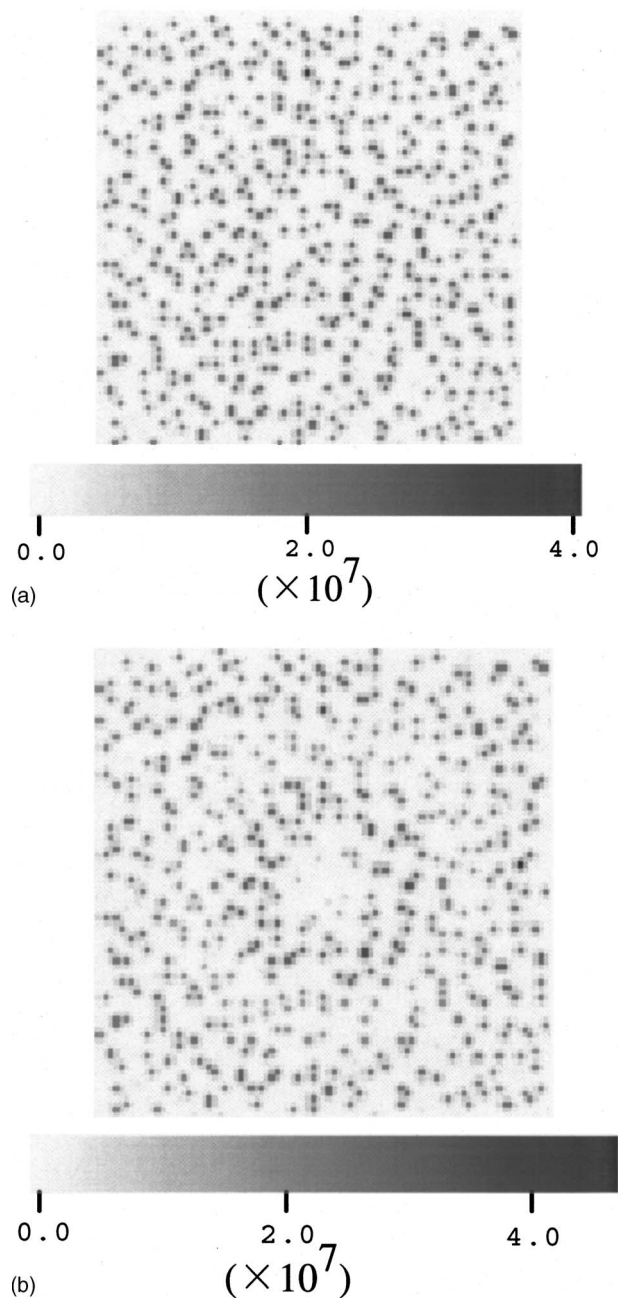


FIG. 4. The reconstructed images after 4500 iterations [(a) with  $F_N=1$  and (b) with  $F_N=10$ ].

destructive interference near the optical axis causes strong artifacts as seen in Fig. 4(b). The uniformity of the illumination wave over the whole area of the specimen was found to be essential for achieving good convergence of the reconstruction. Aside from the extreme proximity case ( $F_N=1000$ ), the most reliable phase retrieval was achieved when  $F_N \leq 1$ . This condition is suitable for the three-dimensional (3D) imaging of specimens with large working distance compared to the case of extreme proximity cases. It is better not to choose the case of  $F_N \ll 1$  since the x-ray flux on the specimen is significantly reduced (see Sec. II).

### B. Correlation of reconstruction accuracy with pinhole size

In the previous subsection, a relatively large pinhole (with the radius 2.7 times larger than the size of the speci-

TABLE II. The quality of reconstruction ( $R$  factor and reconstruction error) as a function of the standard deviations of amplitude within the size of the specimen for various size ratio of pinhole radius ( $r$ ) with the specimen size ( $s$ ). The Fresnel number  $F_N$  was fixed to 1 and the reconstruction was terminated after 4500 iterations.

$r/s(r)$	Deviation (ampl, normalized)	$R$ factor	Reconstruction error
5.7(25 $\mu\text{m}$ )	0.016	0.011	0.005
2.7(12 $\mu\text{m}$ )	0.010	0.036	0.003
1.4(6 $\mu\text{m}$ )	0.099	0.272	0.06
0.7(3 $\mu\text{m}$ )	0.191	0.353	0.14

men) produces a uniform illumination wave near the optical axis when  $F_N=1$ . Good reconstruction was obtained at this condition. While keeping the same Fresnel number and the specimen size, the change of the pinhole size will also affect the accuracy of the reconstruction. This effect was examined in this subsection. The pinhole radius was varied from 3 to 25  $\mu\text{m}$  (i.e., between 0.7 and 5.7 times larger than the size of the specimen).

The convergence of the reconstruction was examined when  $F_N=1$ . We observed that the convergence became much worse for the pinhole size smaller than 12  $\mu\text{m}$  (2.7 times larger than the size of the specimen, see Table II and Fig. 5) which is due to the demagnification of the uniform area.

### C. Correlation of reconstruction accuracy with specimen alignment

The reconstruction accuracy is also dependent on the alignment of the specimen, i.e., offset of the specimen from the optical axis. Simulations were done with the position of the specimen (shown in Fig. 1) offset from the optical axis horizontally. The pinhole radius was fixed to be 12  $\mu\text{m}$  and the Fresnel number to be 1. When the alignment error is larger than 2.5  $\mu\text{m}$  (corresponding to 0.2 times the pinhole

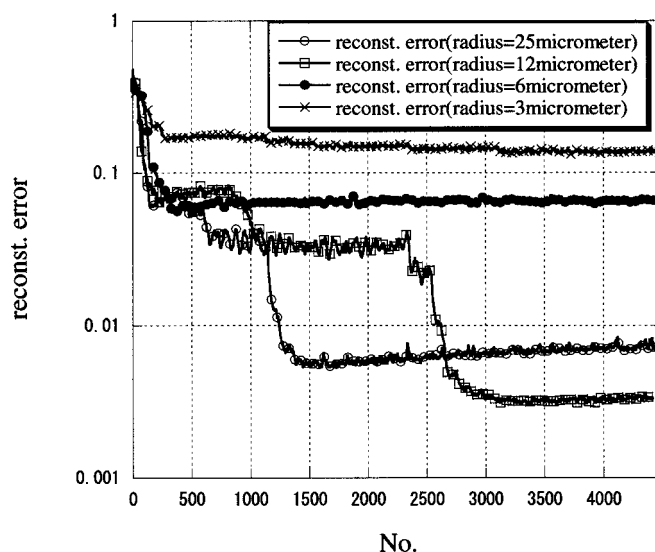


FIG. 5. The reconstruction error as a function of the number of iterations. The convergence of 4500 iterations is shown for the pinhole with radii of 25, 12, 6, and 3  $\mu\text{m}$ , respectively. Fresnel number was fixed to be 1.

TABLE III. The reconstruction error vs the alignment error. The specimen was placed downstream of a  $12\ \mu\text{m}$  radius pinhole with  $F_N=1$ . An offset of 2.5 and  $5\ \mu\text{m}$  from the optical axis was simulated. The reconstruction was terminated after 4500 iterations.

	On axis	Off axis ( $2.5\ \mu\text{m}$ )	Off axis ( $5\ \mu\text{m}$ )
$R$ factor	0.036	0.20	0.30
Reconstruction error	0.003	0.03	0.1

radius, or 0.6 times the specimen size), the convergence degraded severely. The convergence with  $5\ \mu\text{m}$  offset is even much worse than that with  $2.5\ \mu\text{m}$  offset (see Table III and Fig. 6).

#### D. Correlation of the reconstruction accuracy with statistical error

We studied the quality of the phase retrieval as a function of the statistical noise. A plane wave of 8 keV x ray was simulated to illuminate the specimen shown in Fig. 1. No pinhole was considered in this simulation. Poisson noise, a random number between plus and minus one standard deviation of Poisson statistics, was added to each individual pixel of the diffracted intensity ( $I$ ). A half image was centrosymmetrized to produce the full image.

The signal-to-noise-ratio (SNR) was estimated, where the signal and the noise are the original intensity and the added Poisson noise. Since some pixel in the diffracted image ( $I$ ) had a very low count that resulted in a very low SNR, the SNR of an image was evaluated by the 0.01% level from its lowest value. This value,  $\text{SNR}_{\text{min},0.01\%}$ , means that 0.01% of the total number of pixels in the image have lower SNR than this threshold. Numerical constant was multiplied on the image ( $I$ ) to effectively change the Poisson statistics. The convergence at various photon statistics was examined as a function of  $\text{SNR}_{\text{min},0.01\%}$  and was summarized in Table IV and Fig. 7. A very good convergence was achieved with a reconstruction error of  $2 \times 10^{-4}$  after 4500 iterations, which assumes no Poisson noise (i.e., infinite number of photons).

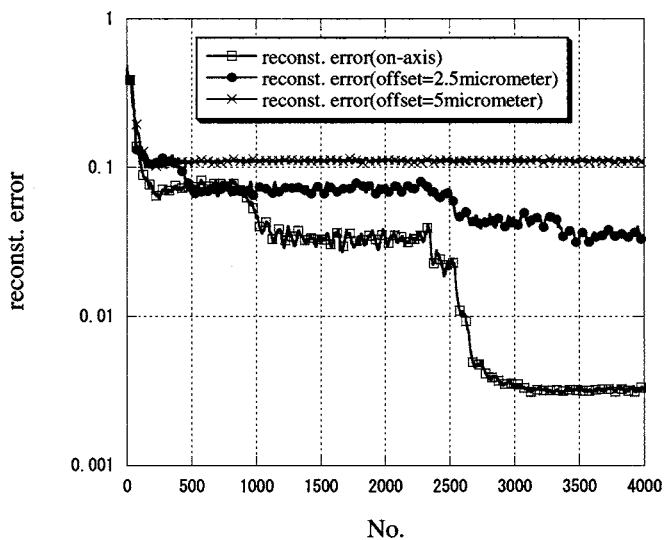


FIG. 6. The reconstruction error as a function of the number of iterations.

TABLE IV. The reconstruction error as a function of  $\text{SNR}_{\text{min},0.01\%}$ . As the reconstruction error function oscillates due to noise, the  $R$  factor was evaluated with an iteration number corresponding to a minimum reconstruction error and an iteration number of 4500, respectively. A plane-wave illumination was assumed.

	$\text{SNR}_{\text{min},0.01\%}$			
	$\infty$	50	5	0.5
$R$ factor	0.0007	0.0009	0.027	0.065
(No. of iterations)	(4500)	(2700)	(1350)	(900)
		0.0006	0.045	0.077
		(4500)	(4500)	(4500)
Minimum reconstruction error	0.0002	0.0011	0.011	0.073
(No. of iterations)	(4400)	(2520)	(1430)	(820)

The quality of reconstruction became worse as the SNR decreased. An  $\text{SNR}_{\text{min},0.01\%}$  of around 5 was needed to achieve the  $R$  factor of less than 5%.

#### V. SUMMARY AND DISCUSSION

The oversampling method with iterative algorithms requires a well-defined illumination wave such as a plane wave. The Fresnel diffraction effect due to a circular pinhole is often neglected in the analysis. By computer simulations we have shown that the distortion of the illumination wave due to the Fresnel diffraction from a pinhole can seriously affect the quality of phase retrieval from the oversampled diffraction patterns. At certain range of conditions, this effect caused strong artifacts in the retrieved images assuming a plane wave for the iterative algorithm. The effect on the accuracy of the phase retrieval was investigated as a function of the Fresnel number, pinhole size, alignment error, and photon statistics.

By varying the Fresnel number, the best quality phase retrieval was obtained with the extreme proximity case and a relatively large pinhole-radius/specimen size ratio. The experimental setup with Fresnel number of around 1 and smaller than 1 also provided high-quality phase retrieval

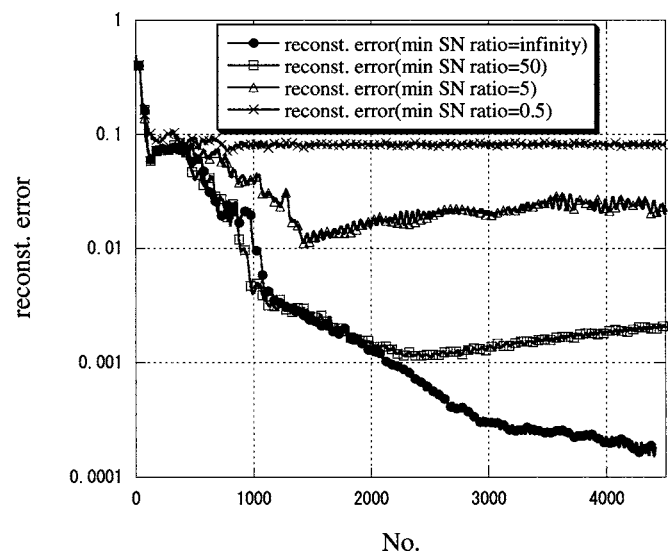


FIG. 7. The reconstruction error as a function of the number of iterations. A plane-wave illumination was assumed.

when the pinhole radius is larger than a few times the specimen size. These conditions may be especially suitable for the 3D image reconstruction with a large working distance. The quality of phase retrieval was found to be severely affected by alignment error and by Poisson noise as well. Since no illumination wave is perfectly well defined, simulations are necessary for reducing reconstruction artifacts in the 3D imaging of materials science samples and biological systems using the third generation synchrotron radiation and future brighter x-ray sources.

- <sup>1</sup>J. Miao, P. Charalambous, J. Kirz, and D. Sayre, *Nature (London)* **400**, 342 (1999).
- <sup>2</sup>I. K. Robinson, I. A. Vartanyants, G. J. Williams, M. A. Pfeifer, and J. A. Pitney, *Phys. Rev. Lett.* **87**, 195505 (2001).
- <sup>3</sup>J. Miao, T. Ishikawa, B. Johnson, E. H. Anderson, B. Lai, and K. O. Hodgson, *Phys. Rev. Lett.* **89**, 088303 (2002).
- <sup>4</sup>S. Marchesini, H. He, H. N. Chapman, S. P. Hau-Riege, A. Noy, M. R. Howells, U. Weierstall, and J. C. H. Spence, *Phys. Rev. B* **68**, 140101 (2003).
- <sup>5</sup>K. A. Nugent, A. G. Peele, H. N. Chapman, and A. P. Mancuso, *Phys. Rev. Lett.* **91**, 203902 (2003).
- <sup>6</sup>G. J. Williams, M. A. Pfeifer, I. A. Vartanyants, and I. K. Robinson, *Phys. Rev. Lett.* **90**, 175501 (2003).
- <sup>7</sup>H. He, S. Marchesini, M. R. Howells, U. Weierstall, H. N. Chapman, S. Hau-Riege, A. Noy, and J. C. H. Spence, *Phys. Rev. B* **67**, 174114 (2003).
- <sup>8</sup>S. Eisebitt, M. Lorgen, W. Eberhardt, J. Luning, S. Andrews, and J. Stohr, *Appl. Phys. Lett.* **84**, 3373 (2004).
- <sup>9</sup>J. Miao, T. Ishikawa, E. H. Anderson, and K. O. Hodgson, *Phys. Rev. B* **67**, 174104 (2003).
- <sup>10</sup>Q. Shen, I. Bazarov, and P. Thibault, *J. Synchrotron Radiat.* **11**, 432 (2004).
- <sup>11</sup>K. Hirano, *Trans. Mater. Res. Soc. Jpn.* **28**, 43 (2003).
- <sup>12</sup>J. Arthur *et al.*, Linac Coherent Light Source (LCLS), Conceptual Design Report (2002), <http://www-ssl.slac.stanford.edu/lcls/cdr>.
- <sup>13</sup>R. Brinkman, G. Materlik, J. Rossbach, and A. Wagner, Conceptual Design Report of a 500 GeV  $e^+e^-$  Linear Collider with Integrated X-ray Laser Facility (1997), [http://tesla.desy.de/new\\_pages/TDR\\_CD/](http://tesla.desy.de/new_pages/TDR_CD/)
- <sup>14</sup>T. Shintake, AIP Conf. Proc. 705, 117 (2004), <http://www-xfel.spring8.or.jp/scss/>
- <sup>15</sup>D. Sayre, *Acta Crystallogr.* **5**, 843 (1952).
- <sup>16</sup>J. Miao, D. Sayre, and H. N. Chapman, *J. Opt. Soc. Am. A* **15**, 1662 (1998).
- <sup>17</sup>R. W. Gerchberg and W. O. Saxton, *Optik (Stuttgart)* **35**, 237 (1972).
- <sup>18</sup>J. R. Fienup, *Opt. Lett.* **3**, 27 (1978).
- <sup>19</sup>M. Born and E. Wolf, *Principles of Optics* (Pergamon, New York, 1964).
- <sup>20</sup>J. W. Goodman, *Introduction to Fourier Optics* (McGraw-Hill, New York, 1968).
- <sup>21</sup>J. R. Fienup, *J. Opt. Soc. Am. A* **4**, 118 (1987).
- <sup>22</sup>Y. Nishino, J. Miao, and T. Ishikawa, *Phys. Rev. B* **68**, 220101 (2003).
- <sup>23</sup>J. Miao, Y. Nishino, Y. Kohmura, B. Johnson, C. Song, S. H. Risbud, and T. Ishikawa, *Phys. Rev. Lett.* **95**, 085503 (2005).